



# Structural verification of a tetrahydrotetrazole compound

Gary W. Breton,\* Lauren A. Hahn and Kenneth L. Martin

Department of Chemistry and Biochemistry, Berry College, Mount Berry, GA 30149-5036, USA. \*Correspondence e-mail: gbreton@berry.edu

Received 8 May 2019

Accepted 17 July 2019

Edited by H. Uekusa, Tokyo Institute of Technology, Japan

**Keywords:** tetrahydrotetrazole; tetrazolidine; azimine; azo imide; crystal structure; azomethine imide.

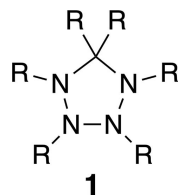
**CCDC reference:** 1941061

**Supporting information:** this article has supporting information at journals.iucr.org/c

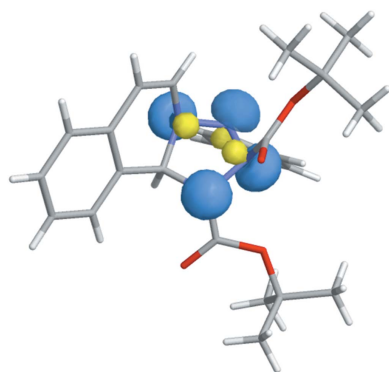
Tetrahydrotetrazoles are five-membered-ring heterocycles containing four contiguous saturated nitrogen atoms. Very few examples of such compounds have been reported in the literature. Our previous attempt at the synthesis of a member of this class of compound suggested that the N—N bonds may be more labile than expected. This finding raised the question as to whether the structures of any of the previously reported tetrahydrotetrazoles had been properly assigned. We have reproduced the synthesis of a reported tetrahydrotetrazole, namely 1,2-di-*tert*-butyl 3-phenyl-1*H*,2*H*,3*H*,10*bH*-[1,2,3,4]tetrazolo[5,1-*a*]isoquinoline-1,2-dicarboxylate, C<sub>25</sub>H<sub>30</sub>N<sub>4</sub>O<sub>4</sub>, and have now confidently confirmed its structure *via* X-ray crystallography. However, while sufficiently stable in the crystal phase, we discovered that it remains very labile in solution (having a half-life of only 15 min at 20 °C in CDCl<sub>3</sub>). A tentative reaction pathway for its dissociation based on <sup>1</sup>H NMR spectral evidence is provided.

## 1. Introduction

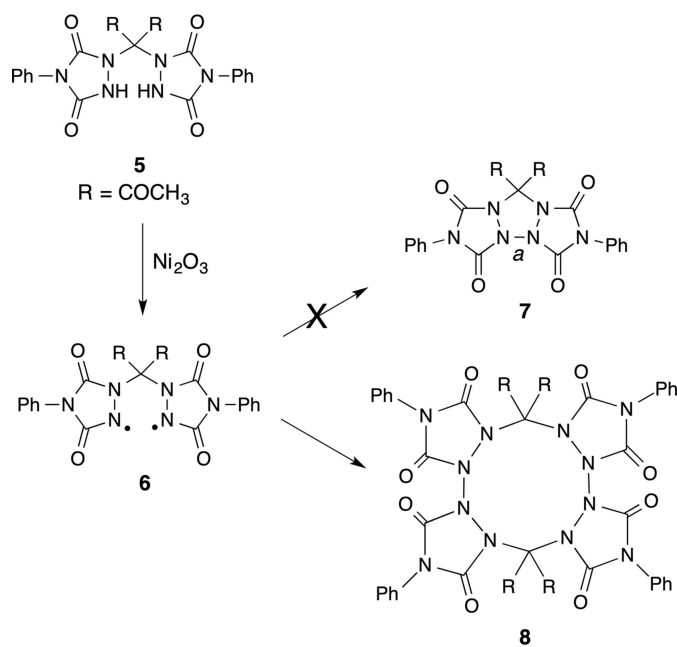
We recently investigated and reported upon a potential synthetic route towards a little-investigated class of compounds known as the tetrahydrotetrazoles (**1**) (Breton & Martin, 2018). These compounds are characterized by having single bonds between four contiguous saturated nitrogen atoms present within a five-membered ring. Unlike carbon, its neighbor in the periodic table, catenation of N atoms is disfavored (Légaré *et al.*, 2019; Tang *et al.*, 2013; Zhang & Shreeve, 2013). Thus, it is not surprising that very few examples of tetrahydrotetrazoles have been reported in the literature (see representative examples in Fig. 1) (Bast *et al.*, 1998; Exner *et al.*, 2000; Krageloh *et al.*, 1984; Ostrovskii *et al.*, 2008; Tokitoh *et al.*, 1989).



In a previous report, we related our attempt to synthesize a novel tetrahydrotetrazole by oxidization of the readily available 1,1-bisurazole **5** (see Scheme 1) (Breton & Martin, 2018). We unexpectedly found that rather than yielding the desired tetrahydrotetrazole **7**, the proposed diradicaloid intermediate **6** instead favored formation of the larger ten-membered ring system **8**, the structure of which was confirmed by X-ray crystallography. Theoretical calculations confirmed the susceptibility of the central N—N bond of **7** (labelled *a* in Scheme 1) towards cleavage and, therefore, its propensity to favor formation of **8**. This work put into question whether the



previously reported tetrahydrotetrazole **2**, whose structure closely resembles that of **7**, indeed had the structure as assigned in the literature. In addition, because all of the reported tetrahydrotetrazoles share a similar central N–N bond, we wondered whether the structure of *any* tetrahydrotetrazole that had been reported in the literature was correct since none of the structures had been corroborated *via* X-ray crystallographic analysis. Unfortunately, tetrahydrotetrazole **2** was obtained in low yield as a by-product from a reaction pathway that would have been difficult to reproduce. On the other hand, tetrahydrotetrazole **3** appeared to be a readily accessible synthetic target. Interestingly, the authors of the original report were only comfortable assigning the structure of **3** as being ‘highly probable’ (Bast *et al.*, 1998). Given this uncertainty, along with the fact that **3** was characterized as a crystalline solid, and therefore likely amenable to X-ray crystallographic analysis, we selected **3** as a viable candidate for structural confirmation of the tetrahydrotetrazole framework.



## 2. Experimental

Unless otherwise specified, all reagents and solvents were purchased from commercial sources and used without further treatment or purification.  $^1\text{H}$  and  $^{13}\text{C}$  NMR spectra were collected at 400 and 100 MHz, respectively, in  $\text{CDCl}_3$  as solvent. Compounds **9** (Barbier *et al.*, 1996) and **10** (Bast *et al.*, 1998) were prepared as described previously. X-ray diffraction data were collected at Emory University’s X-ray Crystallography Center on a Rigaku XtaLAB Synergy-S diffractometer with a HyPix-6000HE Hybrid Photon Counting detector.

### 2.1. Synthesis of **3**

As illustrated in Scheme 2, to compound **10** (0.5 g, 1.95 mmol) in distilled  $\text{H}_2\text{O}$  (5 ml) was added  $\text{Na}_2\text{CO}_3$  (0.23 g,

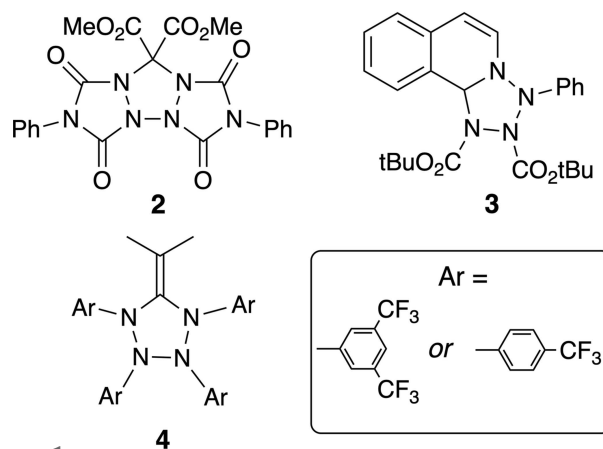


**Figure 1**  
The structures of **2** (Tokitoh *et al.*, 1989), **3** (Bast *et al.*, 1998), and **4** (Krageloh *et al.*, 1984) as representative examples of tetrahydrotetrazoles previously reported in the literature.

2.16 mmol, 1.1 equiv.) as a solution in  $\text{H}_2\text{O}$  (2 ml). The mixture became dark immediately and thickened with a precipitate of **11**. The mixture was stirred manually with a spatula for 10 min, and then washed four times with  $\text{CS}_2$  (2 ml). The organic solution was dried over  $\text{Na}_2\text{SO}_4$  and filtered. To the resulting deep-red–brown solution was added solid di-*tert*-butyl azodicarboxylate (0.4 g, 0.9 equiv.) immediately. The solution became pale-yellow–orange in color. A sample of the solution was subjected to  $^1\text{H}$  NMR spectroscopic analysis (in  $\text{CS}_2$  as solvent), which showed the expected product **3**, along with some unreacted azodicarboxylate compound. The  $\text{CS}_2$  solvent was removed by blowing dry  $\text{N}_2$  over the solution until a crystalline material was obtained. The solid was dissolved in diethyl ether (20 ml), followed by the slow addition of petroleum ether (20 ml). The resulting solution was placed in a freezer until crystals formed. The solvent was removed using a pipette, and the crystals rinsed with cold petroleum ether to afford **3** as pale-yellow–orange blocks (stored at  $-10^\circ\text{C}$ ) (m.p.  $96^\circ\text{C}$ ). IR (solid,  $\text{cm}^{-1}$ ): 763, 779, 803, 1154, 1291, 1320, 1488, 1594, 1646, 1715, 1752;  $^1\text{H}$  NMR ( $\text{CDCl}_3$ ,  $-20^\circ\text{C}$ ):  $\delta$  7.87 (*br d*,  $J = 6.2$  Hz, 1H), 7.40 (*d*,  $J = 8.1$  Hz, 2H), 7.32 (*t*,  $J = 7.4$  Hz, 2H), 7.29 (*d*,  $J = 7.4$  Hz, 1H), 7.20 (*t*,  $J = 7.4$  Hz, 1H), 7.11 (*t*,  $J = 7.4$  Hz, 1H), 7.05 (*d*,  $J = 7.4$  Hz, 1H), 6.49 (*d*,  $J = 8.1$  Hz, 1H), 5.78 (*s*, 1H), 5.76 (*d*,  $J = 8.1$  Hz, 1H), 1.43 (*s*, 18H);  $^{13}\text{C}$  NMR ( $\text{CDCl}_3$ ,  $-30^\circ\text{C}$ ):  $\delta$  156.3, 146.2, 134.0, 130.7, 129.4, 129.2, 129.0, 126.7, 126.5, 125.1, 124.8, 117.5, 107.6, 83.2, 81.9, 72.1, 28.0, 27.7. The NMR spectra are provided in the supporting information. The crystals formed from this method were suitable for X-ray crystallographic analysis.

### 2.2. Dissociation of compound **3** in $\text{CDCl}_3$

As illustrated in Scheme 3, compound **3** (30 mg, 0.07 mmol) was dissolved in  $\text{CDCl}_3$  (0.5 ml) at room temperature and quickly inserted into the temperature-controlled probe of the NMR spectrometer maintained at  $20^\circ\text{C}$ . A  $^1\text{H}$  NMR spectrum was obtained every 5 min until loss of the signals for **3** was observed (approximately 1 h). Signals for isoquinoline were observed along with signals attributed to azo imide **13**.  $^1\text{H}$

**Table 1**  
Experimental details of **3**.

Crystal data	
Chemical formula	C <sub>25</sub> H <sub>30</sub> N <sub>4</sub> O <sub>4</sub>
<i>M<sub>r</sub></i>	450.53
Crystal system, space group	Monoclinic, <i>P</i> <sub>2</sub> <sub>1</sub> / <i>c</i>
Temperature (K)	90
<i>a</i> , <i>b</i> , <i>c</i> (Å)	9.2613 (19), 10.882 (2), 23.583 (5)
β (°)	95.54 (3)
<i>V</i> (Å <sup>3</sup> )	2365.7 (8)
<i>Z</i>	4
Radiation type	Mo <i>K</i> α
μ (mm <sup>-1</sup> )	0.09
Crystal size (mm)	0.54 × 0.33 × 0.28
Data collection	
Diffractometer	XtaLAB Synergy Dualflex HyPix
Absorption correction	Gaussian ( <i>CrysAlis PRO</i> ; Rigaku OD, 2018)
<i>T<sub>min</sub></i> , <i>T<sub>max</sub></i>	0.372, 1.000
No. of measured, independent and observed [ <i>I</i> > 2σ( <i>I</i> )] reflections	183544, 24326, 19422
<i>R<sub>int</sub></i>	0.036
(sin θ/λ) <sub>max</sub> (Å <sup>-1</sup> )	1.075
Refinement	
<i>R</i> [ <i>F</i> <sup>2</sup> > 2σ( <i>F</i> <sup>2</sup> )], <i>wR</i> ( <i>F</i> <sup>2</sup> ), <i>S</i>	0.042, 0.116, 1.04
No. of reflections	24326
No. of parameters	418
H-atom treatment	All H-atom parameters refined
Δρ <sub>max</sub> , Δρ <sub>min</sub> (e Å <sup>-3</sup> )	0.71, -0.25

Computer programs: *CrysAlis PRO* (Rigaku OD, 2018), *SHELXT* (Sheldrick, 2015a), *SHELXL2017* (Sheldrick, 2015b) and *OLEX2* (Dolomanov *et al.*, 2009).

NMR (CDCl<sub>3</sub>): δ 7.94 (*br m*, 2H), 7.44 (*t*, *J* = 7.3 Hz, 2H), 7.31 (*t*, *J* = 7.3 Hz, 1H), 1.64 (*s*, 9H), 1.51 (*br s*, 9H). The NMR spectrum is provided in the supporting information. Allowing the above solution to stand at room temperature overnight led to loss of the signals attributed to **13**.

### 2.3. Computational methods

Geometry optimization and energy calculations were performed using *GAUSSIAN16* software (Frisch *et al.*, 2016) employing the M062X functional and 6-311G(d,p) basis set. Analysis of the vibrational frequencies for the optimized structures confirmed the absence of imaginary frequencies for the ground-state structures. Natural bond orbital (NBO) calculations were carried out with the *NBO6* program at the B3LYP/6-31G(d) level of theory (Glendening *et al.*, 2013). Additional details for the optimized structures are provided in the supporting information.

### 2.4. Refinement

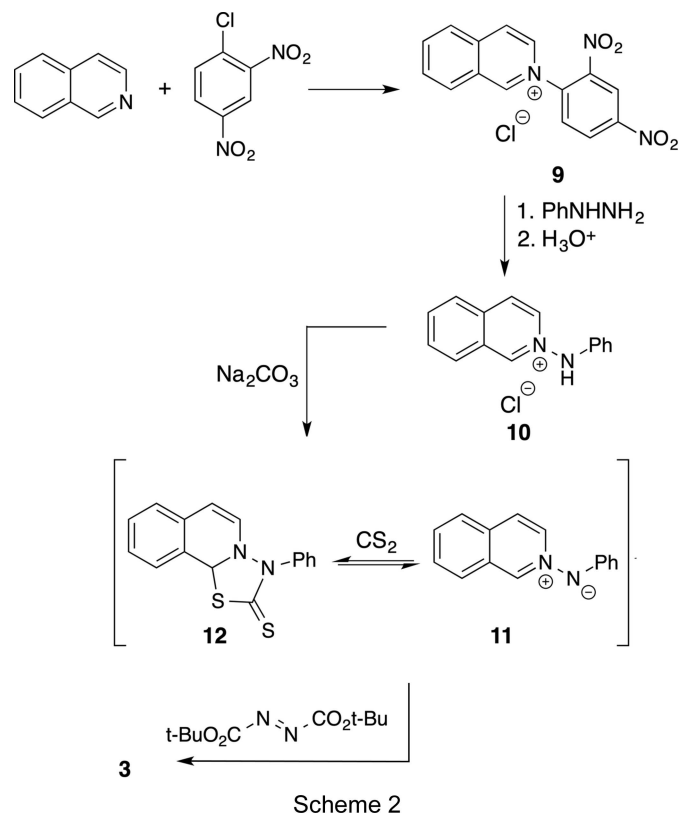
Crystal data, data collection and structure refinement details are summarized in Table 1. H atoms were refined as unconstrained atoms with individual isotropic displacement parameters.

## 3. Results and discussion

### 3.1. Synthesis

The synthesis of compound **3** generally followed previous reports from the literature (see Scheme 2) (Barbier *et al.*, 1996;

Bast *et al.*, 1998). Heating isoquinoline with 1-chloro-2,4-dinitrobenzene led to the formation of the *N*-(2,4-dinitrophenyl)isoquinolinium chloride salt, **9**. Treatment of **9** with phenyl hydrazine followed by acid-catalyzed hydrolysis afforded 2-anilinoisoquinolinium salt **10**, as reported. Salt **10** serves as the immediate precursor to azomethine imide **11** *via* deprotonation with Na<sub>2</sub>CO<sub>3</sub> in water. We extracted the deep-red-brown zwitterion **11** into carbon disulfide, which formed the CS<sub>2</sub> adduct **12** (this was confirmed by <sup>1</sup>H NMR analysis relative to the spectrum reported in the literature). The solution remained deeply colored, however, suggesting that at least some free **11** remains available for further reaction (see Scheme 2). Therefore, instead of isolating adduct **12** as described in the literature, we instead simply added 0.9 equivalents of di-*tert*-butyl azodicarboxylate directly to the CS<sub>2</sub> solution, which quickly quenched the characteristic color of the imide to form an adduct, presumably that of compound **3**. The CS<sub>2</sub> was removed with a gentle stream of dry nitrogen gas and the resulting solid taken up in a 1:1 (*v/v*) mixture of ether and petroleum ether. This solution was placed in a freezer until the adduct crystallized as pale-yellow blocks. The melting point, IR spectrum, and <sup>1</sup>H NMR spectrum (see below for further discussion) agreed with the literature data, confirming the synthesis of the previously reported adduct.



### 3.2. X-ray crystallographic analysis

Crystals of **3** grown from a mixture of ether and petroleum ether at -10 °C as described in the *Experimental* section (§2) were suitable for X-ray crystallographic analysis. A displacement ellipsoid diagram is provided in Fig. 2(a). The X-ray

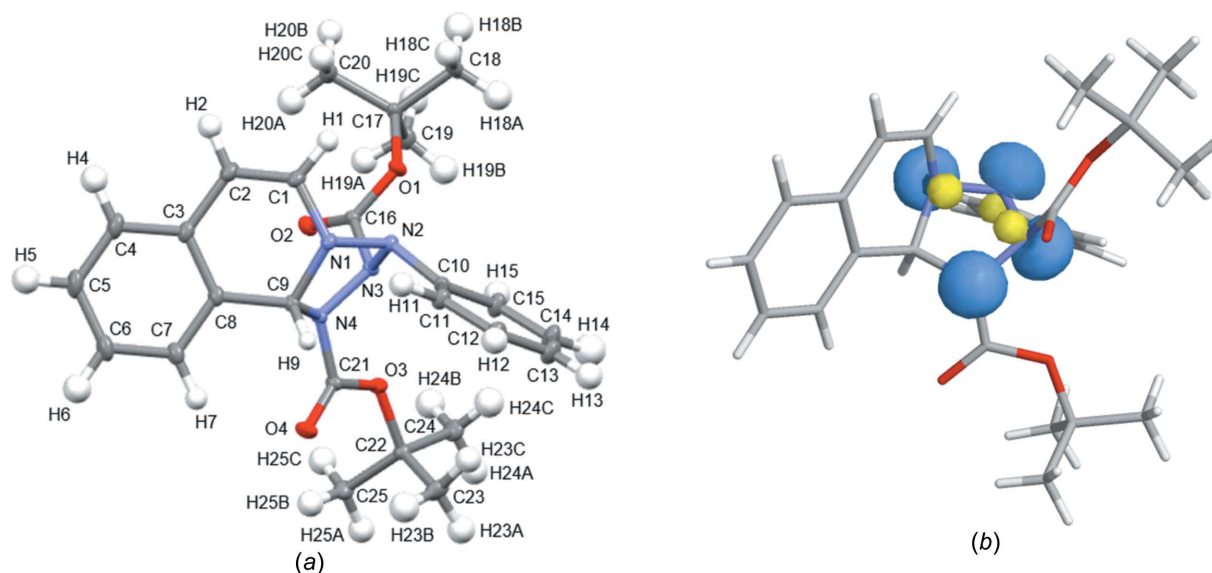


Figure 2

(a) Displacement ellipsoid diagram for compound **3**, with non-H atoms drawn at the 50% probability level. (b) Spatial placement of the N-atom lone pairs (colored blue) of **3**, as predicted by NBO calculations.

structure confirmed the presence of the tetrahydrotetrazole ring within the structure of **3**. Note that as far as we know, this is the first published crystal structure of a tetrahydrotetrazole ring system. Four singly-bonded N atoms are clearly evident in the structure. The N atoms adopt a conformation relative to one another so as to minimize destabilizing repulsive interactions from neighboring lone pairs. This is readily visualized from the results of a natural bond orbital (NBO) calculation on the crystal structure geometry carried out at the B3LYP/6-31G(d) level of theory (see Fig. 2b). Of particular interest are the lengths of the five bonds defining the tetrahydrotetrazole ring embedded within the structure of **3** (see Fig. 3). According to the National Institute of Standards and Technology (Johnson, 2018), hydrazine has an N–N bond length of 1.446 Å. The N1–N2 and N2–N3 bonds in tetrahydrotetrazole **3** are similar in length, but somewhat shorter than that of hydrazine. The N3–N4 bond is the shortest of the three N–N bonds, but all three are relatively close in value (differences of 0.0136 and 0.0131 Å from the N1–N2 and N2–N3 bonds, respectively). In particular, the central N2–N3 bond shows no indication of being particularly strained or prone to rupture. According to the same source, a C–N bond has an average length of 1.421 Å and generally ranges from 1.35 to 1.49 Å. Thus, the C9–N1 bond of **3** is somewhat long relative to the average, but falls within the typical bond-length range. Notably, however, the C9–N4 bond is not only considerably longer ( $\Delta = 0.09$  Å) than the average C–N bond length, but also significantly exceeds the sum of the atomic radii (1.47 Å). To ensure that the long bond was not an artefact of crystal packing forces, we optimized the geometry of compound **3** computationally at the M062X/6-311G(d) level of theory using the coordinates from the crystal structure geometry as initial input. The computationally derived bond lengths are compared to the experimentally derived bond lengths in Fig. 3. Generally, there is good agreement between

the two sets of data ( $\pm 0.01$  Å), and the same trend in relative bond lengths is observed. In particular, the long C9–N4 bond is retained in the computationally obtained *in vacuo* geometry. Long bonds are often indicative of strain within a molecule (Liebman & Greenberg, 1976). For compound **3**, the long bond could conceivably act to relieve some of the steric interaction between the *tert*-butyl carboxylate group on atom N3 and the isoquinoline ring system.

### 3.3. Studies on the stability of tetrahydrotetrazole 3

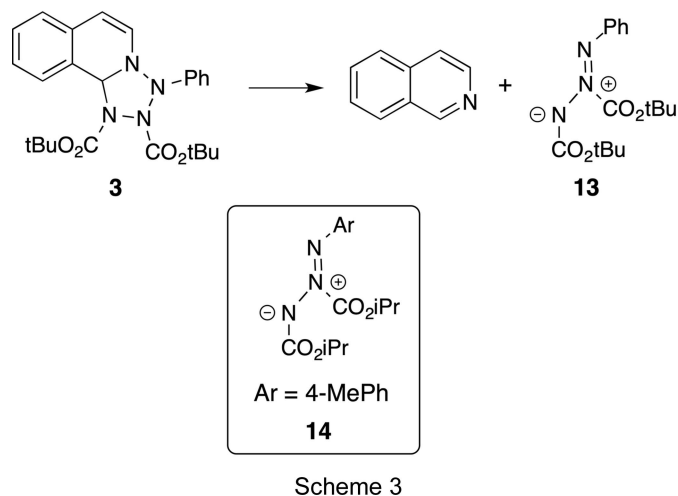
Compound **3** was stable in crystalline form even at room temperature (at least for short periods of time), but it was observed to be much less stable in solution. Dissolution of the pale-yellow crystals of **3** in CDCl<sub>3</sub> at room temperature resulted in rapid formation of the deep-red-brown color characteristic of azomethine imide **11**, suggesting some retrocycloaddition of adduct **3**. Indeed, in the original report on **3**, it was indicated that formation of a deeply colored solution upon warming an originally colorless solution of **3** was reversible upon cooling (Bast *et al.*, 1998). In agreement with the authors, we found that if a CDCl<sub>3</sub> solution of the product is prepared at room temperature, the deep-red color that immediately formed was lost upon cooling the solution to

	Experimental	Computational
C9–N1	1.4699(7)	1.472
C1–N4	1.5086(6)	1.502
N1–N2	1.4282(6)	1.422
N2–N3	1.4277(6)	1.413
N3–N4	1.4146(6)	1.402

Figure 3

Relevant experimentally and computationally [M062X/6-311G(d)] derived bond lengths (Å) for the tetrahydrotetrazole ring of compound **3**.

−10 °C. There were not significant amounts of di-*tert*-butyl azodicarboxylate present in the <sup>1</sup>H NMR spectrum, however, so the extent of retro-cycloaddition must be very limited. We learned that if a solution of **3** was prepared and maintained at −10 °C, the color attributed to **11** did not form. When this cold solution was transferred directly to the pre-cooled (−20 °C) probe of the magnet for NMR analysis, a clean <sup>1</sup>H NMR spectrum corresponding to that previously reported for **3** could be collected.



If a cold solution of **3** was warmed and then maintained at 20 °C, however, loss of signals attributed to **3** was observed in the <sup>1</sup>H NMR spectrum. Concurrently, the growth of signals attributed to isoquinoline and a new compound were observed. The half-life for this reaction was estimated to be a relatively fast 15 minutes, as determined by <sup>1</sup>H NMR spectroscopy. The new compound that forms is apparently not stable, and undergoes further decomposition upon standing in solution at room temperature to ultimately afford a complex mixture of products. This interesting solution-phase behavior was not reported in the initial report (Bast *et al.*, 1998). Provided the clue that isoquinoline was formed from decomposition of **3** in solution, we speculated that the new compound formed is the azo imide **13** (Scheme 3). The <sup>1</sup>H NMR signals for the secondary compound were consistent with proposed structure **13**: aromatic protons consisting of a broad downfield multiplet at 7.94 ppm (2H), a triplet at 7.41 ppm (2H) and a triplet at 7.31 ppm (1H), and inequivalent *tert*-butyl signals at 1.64 and 1.51 ppm (broadened). The broadening of some signals is likely due to the hindered rotation of the phenyl and *tert*-butyl groups in the sterically-congested environment. An azo imide similar to **13** has been reported previously (**14**; see Scheme 3), and its susceptibility to decomposition upon standing at room temperature, similar to the decomposition of the proposed azo imide **14**, was noted (Egger *et al.*, 1983). The dissociation process is likely favored by relief of the internal molecular strain that resulted in the formation of the long C–N bond observed in the structure of **3**. Calculations at the M062X/6-311G(d,p) level of theory on **3**, isoquinoline, and **13** predict a favorable change in free energy ( $\Delta G = -17.9$  kcal mol<sup>−1</sup>) for the decomposition process.

## 4. Conclusions

The structure of compound **3**, as proposed earlier in the literature, has been confirmed by X-ray crystallography to be that of a tetrahydrotriazole. We believe this is the first crystallographic verification of this unique heterocyclic ring system. A particularly interesting revelation from the X-ray analysis was the observation of an unusually long C–N bond in the structure. <sup>1</sup>H NMR spectroscopy studies confirm that compound **3** undergoes dissociation in solution to form isoquinoline and a secondary compound. NMR data and theoretical calculations support the assignment of the secondary compound as azo imide **13**.

## Acknowledgements

GWB and KLM thank Berry College for providing financial support for this project, and thank Dr John Bacsá, Facilities Director of Emory University's X-ray Crystallography Center (supported by the National Science Foundation under CHE-1626172), for collecting the X-ray crystal data on compound **3**.

## References

- Barbier, D., Marazano, C., Das, B. C. & Potier, P. (1996). *J. Org. Chem.* **61**, 9596–9598.
- Bast, K., Behrens, M., Durst, T., Grashey, R., Huisgen, R., Schiffer, R. & Temme, R. (1998). *Eur. J. Org. Chem.* **1998**, 379–385.
- Breton, G. W. & Martin, K. L. (2018). *Acta Cryst.* **C74**, 558–563.
- Dolomanov, O. V., Bourhis, L. J., Gildea, R. J., Howard, J. A. K. & Puschmann, H. (2009). *J. Appl. Cryst.* **42**, 339–341.
- Egger, N., Hoesch, L. & Dreiding, A. S. (1983). *Helv. Chim. Acta*, **66**, 1599–1607.
- Exner, K., Fischer, G., Bahr, N., Beckmann, E., Lugan, M., Yang, F., Rihs, G., Keller, M., Hunkler, D., Knothe, L. & Prinzbach, H. (2000). *Eur. J. Org. Chem.* **2000**, 763–785.
- Frisch, M. J., *et al.* (2016). *GAUSSIAN16*. Revision B.01. Gaussian Inc., Wallingford CT, USA. <http://www.gaussian.com>.
- Glendening, E. D., Badenhoop, J. K., Reed, A. E., Carpenter, J. E., Bohmann, J. A., Morales, C. M., Landis, C. R. & Weinhold, F. (2013). *NBO6.0*. Theoretical Chemistry Institute, University of Wisconsin, Madison, USA. <http://nbo6.chem.wisc.edu/>.
- Johnson, R. D. III (2018). Editor. NIST Computational Chemistry Comparison and Benchmark Database, NIST Standard Reference Database Number 101, Release 19, April 2018. <http://cccbdb.NIST.gov/>.
- Krageloh, K., Anderson, G. H. & Stang, P. J. (1984). *J. Am. Chem. Soc.* **106**, 6015–6021.
- Légaré, M. A., Rang, M., Bélanger-Chabot, G., Schweizer, J. I., Krummenacher, I., Bertermann, R., Arrowsmith, M. C., Holt-hausen, M. C. & Braunschweig, H. (2019). *Science*, **363**, 1329–1332.
- Liebman, J. F. & Greenberg, A. (1976). *Chem. Rev.* **76**, 311–365.
- Ostrovskii, V. A., Koldobskii, G. I. & Trifonov, R. E. (2008). *Comprehensive Heterocyclic Chemistry III*, edited by A. R. Katritzky, C. A. Ramsden, E. F. V. Scriven & R. J. K. Taylor, Vol. 6, p. 261. New York: Elsevier.
- Rigaku OD (2018). *CrysAlis PRO*. Rigaku Corporation, Yarnton, Oxfordshire, England.
- Sheldrick, G. M. (2015a). *Acta Cryst.* **A71**, 3–8.
- Sheldrick, G. M. (2015b). *Acta Cryst.* **C71**, 3–8.
- Tang, Y., Yang, H. & Cheng, G. (2013). *Synlett*, **24**, 2183–2187.
- Tokitoh, N., Suzuki, T., Itami, A., Goto, M. & Ando, W. (1989). *Tetrahedron Lett.* **30**, 1249–1252.
- Zhang, Q. & Shreeve, J. M. (2013). *Angew. Chem. Int. Ed.* **52**, 8792–8794.

## supporting information

*Acta Cryst.* (2019). C75, 1208-1212 [https://doi.org/10.1107/S2053229619010210]

## Structural verification of a tetrahydrotetrazole compound

Gary W. Breton, Lauren A. Hahn and Kenneth L. Martin

## Computing details

Data collection: *CrysAlis PRO* (Rigaku OD, 2018); cell refinement: *CrysAlis PRO* (Rigaku OD, 2018); data reduction: *CrysAlis PRO* (Rigaku OD, 2018); program(s) used to solve structure: SHELXT (Sheldrick, 2015a); program(s) used to refine structure: *SHELXL2017* (Sheldrick, 2015b); molecular graphics: OLEX2 (Dolomanov *et al.*, 2009); software used to prepare material for publication: OLEX2 (Dolomanov *et al.*, 2009).

1,2-Di-*tert*-butyl 3-phenyl-1*H*,2*H*,3*H*,10*bH*-[1,2,3,4]tetrazolo[5,1-*a*]isoquinoline-1,2-dicarboxylate*Crystal data*

C<sub>25</sub>H<sub>30</sub>N<sub>4</sub>O<sub>4</sub>

*M<sub>r</sub>* = 450.53

Monoclinic, *P*2<sub>1</sub>/*c*

*a* = 9.2613 (19) Å

*b* = 10.882 (2) Å

*c* = 23.583 (5) Å

$\beta$  = 95.54 (3)°

*V* = 2365.7 (8) Å<sup>3</sup>

*Z* = 4

*F*(000) = 960

*D<sub>x</sub>* = 1.265 Mg m<sup>-3</sup>

Melting point: 369 K

Mo *K* $\alpha$  radiation,  $\lambda$  = 0.71073 Å

Cell parameters from 79687 reflections

$\theta$  = 1.7–49.2°

$\mu$  = 0.09 mm<sup>-1</sup>

*T* = 90 K

Block, colourless

0.54 × 0.33 × 0.28 mm

*Data collection*

XtaLAB Synergy Dualflex HyPix  
diffractometer

Radiation source: micro-focus sealed X-ray  
tube, PhotonJet (Mo) X-ray Source

Mirror monochromator

$\omega$  scans

Absorption correction: gaussian  
(*CrysAlis PRO*; Rigaku OD, 2018)

*T<sub>min</sub>* = 0.372, *T<sub>max</sub>* = 1.000

183544 measured reflections

24326 independent reflections

19422 reflections with *I* > 2 $\sigma$ (*I*)

*R<sub>int</sub>* = 0.036

$\theta_{\max}$  = 49.8°,  $\theta_{\min}$  = 1.7°

*h* = -19→19

*k* = -21→23

*l* = -45→50

*Refinement*

Refinement on *F*<sup>2</sup>

Least-squares matrix: full

*R*[*F*<sup>2</sup> > 2 $\sigma$ (*F*<sup>2</sup>)] = 0.042

*wR*(*F*<sup>2</sup>) = 0.116

*S* = 1.03

24326 reflections

418 parameters

0 restraints

Primary atom site location: dual

Hydrogen site location: difference Fourier map

All H-atom parameters refined

*w* = 1/[ $\sigma^2(F_o^2) + (0.0602P)^2 + 0.2083P$ ]

where *P* = (*F<sub>o</sub>*<sup>2</sup> + 2*F<sub>c</sub>*<sup>2</sup>)/3

( $\Delta/\sigma$ )<sub>max</sub> = 0.003

$\Delta\rho_{\max}$  = 0.71 e Å<sup>-3</sup>

$\Delta\rho_{\min}$  = -0.25 e Å<sup>-3</sup>

*Special details*

**Geometry.** All esds (except the esd in the dihedral angle between two l.s. planes) are estimated using the full covariance matrix. The cell esds are taken into account individually in the estimation of esds in distances, angles and torsion angles; correlations between esds in cell parameters are only used when they are defined by crystal symmetry. An approximate (isotropic) treatment of cell esds is used for estimating esds involving l.s. planes.

*Fractional atomic coordinates and isotropic or equivalent isotropic displacement parameters ( $\text{\AA}^2$ )*

	<i>x</i>	<i>y</i>	<i>z</i>	$U_{\text{iso}}^*/U_{\text{eq}}$
O1	0.27581 (3)	0.73921 (3)	0.78541 (2)	0.01366 (4)
O2	0.42718 (3)	0.60049 (3)	0.83311 (2)	0.01571 (5)
O3	0.31619 (3)	0.67435 (3)	0.96733 (2)	0.01277 (4)
O4	0.20284 (4)	0.49959 (3)	0.99317 (2)	0.01693 (5)
N1	0.02413 (3)	0.52644 (3)	0.82967 (2)	0.01196 (4)
N2	0.05946 (3)	0.65338 (3)	0.83777 (2)	0.01109 (4)
N3	0.20532 (3)	0.65133 (3)	0.86364 (2)	0.01050 (4)
N4	0.21584 (3)	0.54738 (3)	0.89982 (2)	0.01086 (4)
C1	0.06390 (4)	0.48733 (4)	0.77611 (2)	0.01436 (5)
H1	0.0390 (9)	0.5467 (8)	0.7462 (4)	0.0192 (18)*
C2	0.12033 (4)	0.37654 (4)	0.76764 (2)	0.01607 (6)
H2	0.1349 (10)	0.3516 (8)	0.7285 (4)	0.024 (2)*
C3	0.15273 (4)	0.29276 (3)	0.81520 (2)	0.01501 (5)
C4	0.20068 (5)	0.17264 (4)	0.80703 (2)	0.01941 (7)
H4	0.2127 (11)	0.1439 (9)	0.7668 (4)	0.030 (2)*
C5	0.22737 (5)	0.09330 (4)	0.85290 (2)	0.02194 (7)
H5	0.2610 (11)	0.0096 (9)	0.8470 (4)	0.032 (2)*
C6	0.20595 (5)	0.13303 (4)	0.90772 (2)	0.02048 (7)
H6	0.2238 (11)	0.0772 (10)	0.9406 (4)	0.033 (2)*
C7	0.15994 (4)	0.25292 (3)	0.91666 (2)	0.01655 (6)
H7	0.1493 (10)	0.2814 (8)	0.9553 (4)	0.0203 (18)*
C8	0.13412 (4)	0.33298 (3)	0.87069 (2)	0.01338 (5)
C9	0.09017 (4)	0.46394 (3)	0.88103 (2)	0.01160 (4)
H9	0.0233 (8)	0.4678 (7)	0.9109 (3)	0.0129 (15)*
C10	-0.03570 (4)	0.71725 (3)	0.87237 (2)	0.01151 (4)
C11	-0.17551 (4)	0.67480 (4)	0.87762 (2)	0.01539 (5)
H11	-0.2052 (10)	0.5941 (9)	0.8611 (4)	0.025 (2)*
C12	-0.27025 (5)	0.74630 (4)	0.90630 (2)	0.01872 (6)
H12	-0.3665 (11)	0.7162 (9)	0.9081 (4)	0.029 (2)*
C13	-0.22630 (5)	0.85958 (4)	0.92885 (2)	0.02054 (7)
H13	-0.2939 (11)	0.9094 (9)	0.9488 (4)	0.030 (2)*
C14	-0.08583 (5)	0.90087 (4)	0.92372 (2)	0.02242 (8)
H14	-0.0504 (12)	0.9823 (10)	0.9386 (5)	0.042 (3)*
C15	0.00991 (5)	0.82997 (4)	0.89583 (2)	0.01805 (6)
H15	0.1076 (11)	0.8593 (9)	0.8916 (4)	0.028 (2)*
C16	0.31477 (4)	0.65636 (3)	0.82525 (2)	0.01128 (4)
C17	0.37557 (4)	0.77151 (3)	0.74242 (2)	0.01410 (5)
C18	0.29049 (5)	0.86999 (4)	0.70787 (2)	0.02097 (7)
H18A	0.2746 (11)	0.9417 (10)	0.7332 (4)	0.034 (2)*

H18B	0.3474 (11)	0.9002 (10)	0.6766 (4)	0.035 (2)*
H18C	0.2004 (10)	0.8343 (9)	0.6905 (4)	0.027 (2)*
C19	0.51594 (5)	0.82367 (5)	0.77147 (2)	0.02137 (7)
H19A	0.5774 (10)	0.7599 (9)	0.7902 (4)	0.028 (2)*
H19B	0.4928 (11)	0.8866 (9)	0.8007 (4)	0.033 (2)*
H19C	0.5667 (12)	0.8615 (9)	0.7433 (4)	0.034 (2)*
C20	0.40079 (6)	0.65914 (4)	0.70642 (2)	0.02022 (7)
H20A	0.4617 (11)	0.6004 (9)	0.7289 (4)	0.032 (2)*
H20B	0.4554 (10)	0.6840 (9)	0.6749 (4)	0.026 (2)*
H20C	0.3125 (10)	0.6246 (9)	0.6886 (4)	0.026 (2)*
C21	0.24080 (4)	0.57102 (3)	0.95807 (2)	0.01159 (4)
C22	0.35314 (4)	0.71857 (3)	1.02605 (2)	0.01257 (5)
C23	0.21485 (5)	0.73970 (5)	1.05462 (2)	0.02044 (7)
H23A	0.2402 (11)	0.7858 (9)	1.0910 (4)	0.031 (2)*
H23B	0.1726 (12)	0.6633 (10)	1.0646 (5)	0.037 (3)*
H23C	0.1452 (10)	0.7857 (9)	1.0287 (4)	0.028 (2)*
C24	0.42713 (5)	0.84033 (4)	1.01594 (2)	0.01948 (6)
H24A	0.4558 (11)	0.8803 (9)	1.0528 (4)	0.030 (2)*
H24B	0.5160 (12)	0.8251 (10)	0.9961 (4)	0.035 (2)*
H24C	0.3600 (12)	0.8944 (10)	0.9927 (5)	0.036 (2)*
C25	0.45844 (5)	0.62985 (4)	1.05809 (2)	0.01855 (6)
H25A	0.4965 (10)	0.6665 (9)	1.0944 (4)	0.028 (2)*
H25B	0.4113 (11)	0.5510 (9)	1.0645 (4)	0.028 (2)*
H25C	0.5397 (11)	0.6167 (9)	1.0358 (4)	0.031 (2)*

Atomic displacement parameters ( $\text{\AA}^2$ )

	$U^{11}$	$U^{22}$	$U^{33}$	$U^{12}$	$U^{13}$	$U^{23}$
O1	0.01323 (9)	0.01518 (10)	0.01316 (9)	0.00325 (7)	0.00428 (7)	0.00513 (7)
O2	0.01207 (9)	0.01753 (11)	0.01774 (10)	0.00354 (8)	0.00256 (8)	0.00487 (8)
O3	0.01592 (10)	0.01261 (9)	0.00963 (8)	-0.00433 (7)	0.00040 (7)	-0.00066 (7)
O4	0.02262 (12)	0.01558 (11)	0.01255 (9)	-0.00587 (9)	0.00139 (8)	0.00363 (8)
N1	0.01166 (9)	0.01191 (10)	0.01202 (9)	0.00010 (7)	-0.00027 (7)	-0.00217 (7)
N2	0.01000 (9)	0.01155 (9)	0.01165 (9)	0.00056 (7)	0.00063 (7)	-0.00086 (7)
N3	0.01013 (9)	0.01134 (9)	0.00999 (8)	-0.00032 (7)	0.00076 (7)	0.00175 (7)
N4	0.01248 (9)	0.01003 (9)	0.00980 (8)	-0.00225 (7)	-0.00029 (7)	0.00090 (7)
C1	0.01354 (12)	0.01697 (13)	0.01221 (11)	0.00117 (10)	-0.00055 (9)	-0.00345 (9)
C2	0.01536 (13)	0.01701 (13)	0.01575 (12)	0.00058 (10)	0.00109 (10)	-0.00531 (10)
C3	0.01249 (11)	0.01263 (12)	0.01995 (13)	-0.00107 (9)	0.00180 (10)	-0.00415 (10)
C4	0.01706 (14)	0.01319 (13)	0.02859 (18)	-0.00098 (10)	0.00533 (13)	-0.00574 (12)
C5	0.01895 (15)	0.01170 (13)	0.0358 (2)	-0.00012 (11)	0.00599 (15)	-0.00189 (13)
C6	0.01834 (15)	0.01174 (13)	0.0312 (2)	-0.00076 (11)	0.00164 (13)	0.00242 (12)
C7	0.01558 (13)	0.01189 (12)	0.02187 (15)	-0.00184 (10)	0.00032 (11)	0.00124 (10)
C8	0.01170 (11)	0.01050 (11)	0.01775 (12)	-0.00152 (8)	0.00054 (9)	-0.00148 (9)
C9	0.01114 (10)	0.01069 (10)	0.01283 (10)	-0.00145 (8)	0.00041 (8)	-0.00070 (8)
C10	0.01197 (10)	0.01124 (10)	0.01148 (10)	0.00070 (8)	0.00191 (8)	0.00019 (8)
C11	0.01255 (11)	0.01596 (13)	0.01807 (13)	-0.00103 (9)	0.00365 (9)	-0.00334 (10)
C12	0.01477 (13)	0.02046 (16)	0.02190 (15)	-0.00054 (11)	0.00680 (11)	-0.00420 (12)

C13	0.01936 (15)	0.01922 (16)	0.02430 (17)	0.00141 (12)	0.00862 (13)	-0.00541 (13)
C14	0.02111 (17)	0.01592 (15)	0.0315 (2)	-0.00126 (12)	0.00915 (15)	-0.00849 (14)
C15	0.01639 (13)	0.01323 (13)	0.02544 (16)	-0.00203 (10)	0.00671 (12)	-0.00486 (11)
C16	0.01117 (10)	0.01158 (10)	0.01117 (10)	0.00015 (8)	0.00149 (8)	0.00151 (8)
C17	0.01572 (12)	0.01339 (12)	0.01403 (11)	0.00324 (9)	0.00582 (9)	0.00371 (9)
C18	0.02573 (18)	0.02020 (16)	0.01822 (14)	0.01002 (14)	0.00849 (13)	0.00857 (12)
C19	0.01873 (15)	0.02050 (16)	0.02546 (18)	-0.00404 (12)	0.00518 (13)	0.00382 (13)
C20	0.02767 (19)	0.01729 (15)	0.01667 (14)	0.00551 (13)	0.00709 (13)	0.00060 (11)
C21	0.01299 (11)	0.01130 (10)	0.01033 (9)	-0.00198 (8)	0.00034 (8)	0.00086 (8)
C22	0.01253 (11)	0.01427 (12)	0.01080 (10)	-0.00043 (9)	0.00060 (8)	-0.00206 (8)
C23	0.01573 (14)	0.02806 (19)	0.01812 (14)	0.00095 (13)	0.00463 (11)	-0.00534 (13)
C24	0.02259 (16)	0.01579 (14)	0.01981 (15)	-0.00553 (12)	0.00075 (12)	-0.00359 (11)
C25	0.01928 (15)	0.02031 (16)	0.01514 (13)	0.00355 (12)	-0.00306 (11)	-0.00109 (11)

*Geometric parameters (Å, °)*

O1—C16	1.3268 (5)	C3—C8	1.4062 (6)
O1—C17	1.4784 (6)	C4—C5	1.3875 (8)
O2—C16	1.2044 (5)	C5—C6	1.3953 (8)
O3—C21	1.3305 (5)	C6—C7	1.3948 (6)
O3—C22	1.4748 (5)	C7—C8	1.3933 (6)
O4—C21	1.2120 (5)	C8—C9	1.5085 (6)
N1—N2	1.4282 (5)	C10—C11	1.3915 (6)
N1—C1	1.4148 (6)	C10—C15	1.3943 (6)
N1—C9	1.4700 (6)	C11—C12	1.3955 (6)
N2—N3	1.4277 (6)	C12—C13	1.3879 (7)
N2—C10	1.4369 (5)	C13—C14	1.3926 (7)
N3—N4	1.4146 (4)	C14—C15	1.3880 (6)
N3—C16	1.4237 (6)	C17—C18	1.5196 (6)
N4—C9	1.5086 (5)	C17—C19	1.5197 (7)
N4—C21	1.3949 (5)	C17—C20	1.5195 (6)
C1—C2	1.3367 (6)	C22—C23	1.5211 (7)
C2—C3	1.4541 (6)	C22—C24	1.5210 (6)
C3—C4	1.3998 (6)	C22—C25	1.5204 (6)
C16—O1—C17	120.13 (3)	C8—C9—N4	113.80 (3)
C21—O3—C22	120.02 (3)	C11—C10—N2	121.12 (4)
N2—N1—C9	105.40 (3)	C11—C10—C15	120.38 (3)
C1—N1—N2	109.53 (3)	C15—C10—N2	118.16 (3)
C1—N1—C9	118.23 (3)	C10—C11—C12	119.47 (4)
N1—N2—C10	113.49 (3)	C13—C12—C11	120.41 (4)
N3—N2—N1	103.72 (3)	C12—C13—C14	119.68 (4)
N3—N2—C10	111.82 (3)	C15—C14—C13	120.44 (4)
N4—N3—N2	106.11 (3)	C14—C15—C10	119.61 (4)
N4—N3—C16	113.73 (3)	O1—C16—N3	108.34 (3)
C16—N3—N2	115.47 (3)	O2—C16—O1	128.61 (4)
N3—N4—C9	107.33 (3)	O2—C16—N3	122.73 (3)
C21—N4—N3	116.22 (3)	O1—C17—C18	102.08 (3)

C21—N4—C9	116.75 (3)	O1—C17—C19	110.10 (4)
C2—C1—N1	122.96 (4)	O1—C17—C20	109.37 (4)
C1—C2—C3	120.32 (4)	C18—C17—C19	110.80 (4)
C4—C3—C2	121.60 (4)	C20—C17—C18	111.58 (4)
C4—C3—C8	119.19 (4)	C20—C17—C19	112.42 (4)
C8—C3—C2	119.21 (4)	O3—C21—N4	110.60 (3)
C5—C4—C3	120.59 (4)	O4—C21—O3	127.75 (3)
C4—C5—C6	119.92 (4)	O4—C21—N4	121.53 (3)
C7—C6—C5	120.18 (4)	O3—C22—C23	109.65 (4)
C8—C7—C6	119.95 (4)	O3—C22—C24	101.79 (3)
C3—C8—C9	120.25 (3)	O3—C22—C25	109.81 (4)
C7—C8—C3	120.14 (4)	C24—C22—C23	110.43 (4)
C7—C8—C9	119.59 (4)	C25—C22—C23	113.77 (4)
N1—C9—N4	102.20 (3)	C25—C22—C24	110.73 (4)
N1—C9—C8	113.65 (3)		
N1—N2—N3—N4	-35.80 (3)	C4—C3—C8—C9	176.78 (3)
N1—N2—N3—C16	91.19 (3)	C4—C5—C6—C7	-1.01 (7)
N1—N2—C10—C11	-23.78 (5)	C5—C6—C7—C8	0.53 (6)
N1—N2—C10—C15	162.85 (3)	C6—C7—C8—C3	0.73 (6)
N1—C1—C2—C3	-4.16 (6)	C6—C7—C8—C9	-177.57 (3)
N2—N1—C1—C2	141.94 (4)	C7—C8—C9—N1	-162.30 (3)
N2—N1—C9—N4	-27.23 (3)	C7—C8—C9—N4	81.25 (5)
N2—N1—C9—C8	-150.29 (3)	C8—C3—C4—C5	1.04 (6)
N2—N3—N4—C9	18.43 (3)	C9—N1—N2—N3	39.42 (4)
N2—N3—N4—C21	-114.35 (4)	C9—N1—N2—C10	-82.14 (4)
N2—N3—C16—O1	42.68 (4)	C9—N1—C1—C2	21.26 (5)
N2—N3—C16—O2	-143.34 (4)	C9—N4—C21—O3	-158.24 (3)
N2—C10—C11—C12	-172.86 (4)	C9—N4—C21—O4	25.47 (5)
N2—C10—C15—C14	172.36 (4)	C10—N2—N3—N4	86.87 (4)
N3—N2—C10—C11	-140.69 (3)	C10—N2—N3—C16	-146.14 (3)
N3—N2—C10—C15	45.94 (4)	C10—C11—C12—C13	0.80 (7)
N3—N4—C9—N1	5.38 (3)	C11—C10—C15—C14	-1.06 (7)
N3—N4—C9—C8	128.33 (3)	C11—C12—C13—C14	-1.24 (8)
N3—N4—C21—O3	-29.91 (4)	C12—C13—C14—C15	0.53 (8)
N3—N4—C21—O4	153.80 (4)	C13—C14—C15—C10	0.62 (8)
N4—N3—C16—O1	165.71 (3)	C15—C10—C11—C12	0.36 (6)
N4—N3—C16—O2	-20.31 (5)	C16—O1—C17—C18	-178.18 (4)
C1—N1—N2—N3	-88.77 (4)	C16—O1—C17—C19	-60.47 (5)
C1—N1—N2—C10	149.67 (3)	C16—O1—C17—C20	63.53 (5)
C1—N1—C9—N4	95.55 (4)	C16—N3—N4—C9	-109.59 (3)
C1—N1—C9—C8	-27.50 (4)	C16—N3—N4—C21	117.63 (4)
C1—C2—C3—C4	174.71 (4)	C17—O1—C16—O2	1.27 (6)
C1—C2—C3—C8	-4.67 (6)	C17—O1—C16—N3	174.78 (3)
C2—C3—C4—C5	-178.34 (4)	C21—O3—C22—C23	-59.09 (5)
C2—C3—C8—C7	177.88 (3)	C21—O3—C22—C24	-176.04 (3)
C2—C3—C8—C9	-3.83 (5)	C21—O3—C22—C25	66.61 (4)
C3—C4—C5—C6	0.21 (7)	C21—N4—C9—N1	137.87 (3)

C3—C8—C9—N1	19.40 (5)	C21—N4—C9—C8	-99.17 (4)
C3—C8—C9—N4	-97.05 (5)	C22—O3—C21—O4	-5.01 (6)
C4—C3—C8—C7	-1.51 (5)	C22—O3—C21—N4	178.99 (3)

---